Inorganica Chimica Acta 363 (2010) 3390–3398

Contents lists available at ScienceDirect

Inorganica Chimica Acta

journal homepage: www.elsevier.com/locate/ica

Manganese(II) complexes of di-2-pyridinylmethylene-1,2-diimine di-Schiff base ligands: Structures and reactivity

Shadrick I.M. Paris [a], Ünige A. Laskay [a], Shengwen Liang [a], Oksana Pavlyuk [a], Steffen Tschirschwitz [b], Peter Lönnecke [b], Mark C. McMills [a], Glen P. Jackson [a], Jeffrey L. Petersen [c], Evamarie Hey-Hawkins [b,*], Michael P. Jensen [a,**]

[a] Department of Chemistry and Biochemistry, Ohio University, Athens, OH 45701, USA
[b] Fakultät für Chemie und Mineralogie, Institut für Anorganische Chemie, Universität Leipzig, Johannisallee 29, D-04103 Leipzig, Germany
[c] C. Eugene Bennett Department of Chemistry, West Virginia University, Morgantown, WV 26506, USA

ARTICLE INFO

Article history:
Received 27 April 2010
Received in revised form 17 June 2010
Accepted 18 June 2010
Available online 25 June 2010

Keywords:
Manganese
Schiff base
Pentagonal bipyramidal
Phosphine
Ethyldiazoacetate
Imine

ABSTRACT

Manganese(II) complexes $[Mn(L)X_2]$ were prepared and characterized, where L is a neutral di-Schiff base ligand incorporating pyridylimine donor arms, including (1*R*,2*R*)-*N*,*N*′-bis(2-pyridylmethylidene)-1,2-diphenylethylenediimine (L^1), (1*R*,2*R*)-*N*,*N*′-bis(6-methyl-2-pyridylmethylidene)-1,2-cyclohexyldiimine (L^2), or (1*R*,2*R*)-, (1*S*,2*S*)- or racemic *N*,*N*′-bis(2-pyridylmethylidene)-1,2-cyclohexyldiimine (L^3), and $X^- = ClO_4^-$ or Cl^-. Product complexes were structurally characterized, specifically including $[Mn(R,R\text{-}L^1)(NCCH_3)_3](ClO_4)_2$, $[Mn(R,R\text{-}L^2)(OH_2)_2](ClO_4)_2$ and racemic $[Mn(L^3)Cl_2]$. The first of these complexes features a heptacoordinate ligand field in a distorted pentagonal bipyramid, and the latter two are hexacoordinate, but retain equatorially monovacant pentagonal bipyramidal structures. Complexes $[Mn(L^3)X_2]$ ($X^- = Cl^-$, ClO_4^-) were reacted with the primary phosphine $FcCH_2PH_2$ ($Fc = -C_5H_4FeC_5H_5$), H_2O and ethyldiazoacetate (EDA). The first two substrates prompted reactivity at a single ligand imine bond, resulting in hydrophosphination and hydrolysis, respectively. Complexes of the derivative ligands were also structurally characterized. Evidence for EDA activation was obtained by electrospray ionization mass spectrometry, but catalytic carbene transfer was not obtained.

© 2010 Elsevier B.V. All rights reserved.

1. Introduction

Transition metal catalysts supported by Schiff base ligands have assumed a prominent role in modern synthesis [1,2]. Perhaps the best known example is the use of chiral chloromanganese(III) salen complexes as catalysts for asymmetric epoxidations of prochiral olefins [3–5]. Distinct advantages of such ligands include their low cost, facile syntheses, and convenient incorporation of inexpensive, chiral 1,2-diamines into the ligand backbone. Moreover, the ligands generally afford air- and moisture-stable complexes.

Compared to the manganese(III) complexes of dianionic salens just described, neutral di-Schiff base ligands incorporating 2-pyridylaldehydes in place of salicylates support divalent manganese(II). The constrained chelate bite resulting from replacement of the exocyclic phenolate oxygen donors with heterocyclic pyridines also alters the complex geometry [6–13]. Such complexes have been explored as chiral oxo atom transfer catalysts [6,12], and also as precatalysts for olefin polymerization [7]. Given the latter as a precedent for low-valent organometallic chemistry, we hypothesized that the dipyridyldiimine Schiff base complexes might support group transfer reactions of softer isolobal fragments of oxene, such as carbenes and phosphinidenes. Manganese-catalyzed cyclopropanation reactions are rare [14–16].

In the present work, we prepared the following ligands according to literature precedent: (1*R*,2*R*)-*N*,*N*′-bis(2-pyridylmethylidene)-1,2-diphenylethylenediimine (L^1, Scheme 1) [17,18]; (1*R*,2*R*)-*N*,*N*′-bis(6-methyl-2-pyridylmethylidene)-1,2-cyclohexyldiimine (L^2) [19,20]; and (1*R*,2*R*)-, (1*S*,2*S*)- and racemic *N*,*N*′-bis(2-pyridylmethylidene)-1,2-cyclohexyldiimine (L^3) [6]. Mn(II) salts (MnX_2, $X^- = Cl^-$, ClO_4^-) were added in a 1:1 stoichiometry to obtain a variety of complexes [6]. $[Mn(R,R\text{-}L^1)(NCCH_3)_3](ClO_4)_2$, $[Mn(R,R\text{-}L^2)(OH_2)_2](ClO_4)_2$ and racemic $[Mn(L^3)Cl_2]$ were structurally characterized. Moreover, exploratory reactions with the air-stable primary phosphine PH_2CH_2Fc (Fc = ferrocenyl, $-C_5H_4FeC_5H_5$) [21] and ethyldiazoacetate (EDA) [22] as potential phosphinidene and carbene precursors were investigated. While indirect evidence for EDA activation was observed by mass spectrometry, group transfer catalysis was not obtained in solution for either precursor. Instead, novel complexes derived from ligand hydrophosphination

* Corresponding author. Tel.: +49 341 9736151; fax: +49 341 9739319.
** Corresponding author. Tel.: +1 740 593 1745; fax: +1 740 593 0148.
E-mail addresses: hey@uni-leipzig.de (E. Hey-Hawkins), jensenm@ohio.edu (M.P. Jensen).

0020-1693/$ - see front matter © 2010 Elsevier B.V. All rights reserved.
doi:10.1016/j.ica.2010.06.041

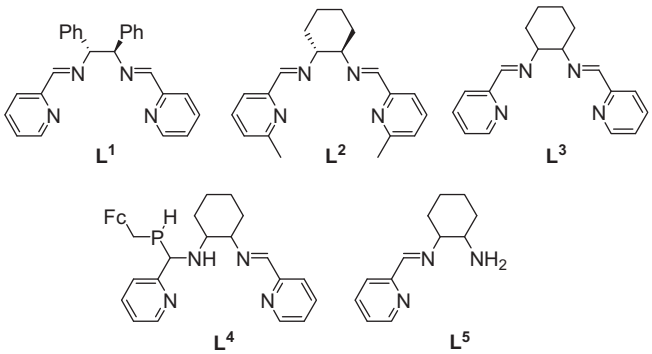

Scheme 1.

(L^4, Scheme 1) and hydrolysis (L^5) were obtained, and these were also structurally characterized.

2. Experimental

All studies were carried out under inert atmosphere using standard techniques. Reagent grade solvents were degassed, dried by standard techniques and distilled before use. The di-Schiff base ligands (Scheme 1) were prepared by 2:1 condensation of 2-picolal or 2-methyl-6-picolal with the appropriate 1,2-diamine in EtOH solution according to literature precedent, and characterized by ^{1}H NMR spectroscopy. Ferrocenylmethylphosphine ($FcCH_2PH_2$) [21] and α-d_1-EDA [23] were prepared by literature procedures. A mixture of ordinary and d_5-EDA was obtained by esterification of glycine in a 1.0:1.2 volume ratio of CH_3CH_2OH and CD_3CD_2OH, followed by diazotization and extraction.

Mass spectrometry was performed on a Thermo Finnigan Polaris Q ion trap with a home-built nano-electrospray ionization source [24]. Polarimetry was performed on an Autopol IV polarimeter with a 10 cm cell. Cyclic voltammetry was performed using a CH Instruments CH1730A potentiostat. ^{1}H and ^{2}H NMR spectra were obtained on a Varian Inova 500 spectrometer. Solution magnetic moments were determined by the Evans NMR method in CD_3OD at 298 K [25]. Elemental analyses were performed by Atlantic Microlabs, Inc. (Norcross, GA).

2.1. [Mn(L^1)(ClO$_4$)$_2$]·H$_2$O

A solution of $Mn(ClO_4)_2{\cdot}6H_2O$ (185 mg, 0.51 mmol) in acetonitrile (5 mL) [*CAUTION:* metal–organic perchlorate salts are potentially explosive!], was added dropwise to a solution of *R*,*R*-L^1 (203 mg, 0.51 mmol) in 5 mL acetonitrile. After stirring 15 min at room temperature, the deep yellow solution was reduced to ca. 2 mL under vacuum, and diethyl ether was added to precipitate the complex as a light-yellow solid. The solid was recovered by filtration, washed with diethyl ether and dried *in vacuo*. Yield: 306 mg, 91%. *Anal.* Calc. for $C_{26}H_{24}Cl_2MnN_4O_9$: C, 47.15; H, 3.65; N, 8.46. Found: C, 47.30; H, 3.55; N, 8.63%. μ_{eff} = 5.6 μ_B. $[\alpha]_d$ = −194.5 (c 1.0, CH_3CN).

2.2. [Mn(L^2)(OH$_2$)$_2$](ClO$_4$)$_2$

Samples of $Mn(ClO_4)_2{\cdot}6H_2O$ (200 mg, 0.55 mmol) and *R*,*R*-L^2 (183 mg, 0.57 mmol) were dissolved separately in CH_3CN (5 mL). The solution of the metal salt was added dropwise to that of the ligand. After stirring 15 min, the solvent was evaporated to yield a light-yellow solid. The product was recovered by filtration, washed with Et_2O and dried. Yield: 316 mg, 94%. *Anal.* Calc. for $C_{20}H_{28}Cl_2MnN_4O_{10}$: C, 39.36; H, 4.62; N, 9.18. Found: C, 39.71; H, 4.40; N, 9.15%. μ_{eff} = 5.7 μ_B. $[\alpha]_d$ = −335.6 (c 1.0, CH_3CN).

2.3. [Mn(L^3)(ClO$_4$)$_2$]·H$_2$O

Complexes of racemic, *R*,*R*- and *S*,*S*-L^3 were prepared by a literature synthesis [6]. *Anal.* Calc. for $C_{18}H_{22}Cl_2MnN_4O_9$: C, 38.32; H, 3.93; N, 9.93. Found: C, 38.32; H, 3.63; N, 9.92%. $[\alpha]_d$ (c 1.0, CH_3CN) = −308.0 (*R*,*R*), +311.0 (*S*,*S*).

2.4. [Mn(L^3)Cl$_2$]·H$_2$O

A solution of $MnCl_2{\cdot}4H_2O$ (451 mg, 2.28 mmol) in methanol (20 mL) was added dropwise to a solution of racemic L^3 (734 mg, 2.51 mmol) in 5 mL acetonitrile. After stirring 45 min, the solution was reduced to 5 mL under vacuum, and diethyl ether was added to precipitate the complex as a yellow solid. The solid was recovered by filtration, washed with diethyl ether and dried *in vacuo*. Yield: 820 mg, 82%. *Anal.* Calc. for $C_{18}H_{22}Cl_2MnN_4O$: C, 49.56; H, 5.08; N, 12.84. Found: C, 49.65; H, 5.18; N, 12.80%. μ_{eff} = 5.6 μ_B.

2.5. [Mn(L^4)(Cl)$_2$]

A 50 mL Schlenk flask was charged with solid samples of racemic $[Mn(L^3)Cl_2]{\cdot}H_2O$ (100 mg, 0.23 mmol) and PH_2CH_2Fc (61 mg, 0.26 mmol). Dichloromethane (15 mL) was added, and the resulting orange solution was stirred at reflux overnight. Solvent was then removed under vacuum until approx. 3 mL remained. Excess diethyl ether was then added, affording a yellow/orange precipitate. The product was washed with diethyl ether (3 × 10 mL) and dried to constant mass. Yield: 150 mg, 94%. *Anal.* Calc. for $C_{29}H_{33}Cl_2FeMnN_4P{\cdot}0.5CH_2Cl_2$: C, 51.15; H, 4.95; N, 8.09. Found: C, 50.86; H, 5.06; N, 8.13%. μ_{eff} = 5.7 μ_B.

2.6. [Mn(L^5)(Cl)$_2$]

$[Mn(L^3)Cl_2]{\cdot}H_2O$ (50 mg, 0.11 mmol) was dissolved in 5 mL MeOH and water was added (0.10 mL). Vapor diffusion of Et_2O afforded orange microcrystalline solids after several days. The product complex $[Mn(L^5)(Cl)_2]$ was recovered by filtration, washed with Et_2O and dried under vacuum to constant mass. Yield: 19 mg (50%). *Anal.* Calc. for $C_{12}H_{17}Cl_2MnN_3$ (**5**): C, 43.79; H, 5.21; N, 12.77. Found: C, 43.65; H, 5.26; N, 12.57%. μ_{eff} = 5.6 μ_B.

2.7. Reaction of [Mn(L^3)(X)$_2$] (X$^-$ = Cl$^-$, ClO$_4^-$) with EDA/styrene

In a typical reaction, racemic $[Mn(L^3)(ClO_4)_2]$ (11.0 mg, 0.020 mmol) was dissolved in acetonitrile (3 mL) and heated to reflux. A solution of ethyldiazoacetate (Aldrich, 1.3 mmol in 5 mL of acetonitrile) combined with styrene (0.6 mL, 5.2 mmol) was added by syringe pump at a rate of 5.9 mL/h. Product distributions were determined by use of an HP 5890 GC–MS equipped with a Restek Corporation model RTX-OPP column. Solvent was removed under vacuum and the residue was purified by flash column chromatography (hexanes/ethyl acetate, 9:1 on silica) to yield a mixture of *trans* and *cis* cyclopropane isomers (R_f = 0.4) and *cis*-ethyl-4-phenylbut-3-enoate (R_f = 0.5). Cyclopropane isomers were then separated on a second column (pentanes/ethyl acetate, 97:3, R_f(*trans*) = 0.5, R_f(*cis*) = 0.4). Enantiomeric excess for isolated cyclopropane isomers was determined by GC–FID techniques using an HP 6890 instrument fitted with a CP-Chirasil-Dex CB column. Isolated products were identified by ^{1}H and ^{13}C NMR spectroscopy in comparison to literature values [26,27]; 3-carboxy-5-phenyl-2-pyrazoline ethyl ester was identified *in situ* by ^{1}H NMR spectroscopy in the absence of metal complex [28]. Alternately, α-d_1-EDA (155 mM), styrene (3.9 equiv.), and metal complex (1.5 mol%) were

combined in solution with d_7-DMF added as an internal standard and heated to reflux under argon; aliquots of the reaction solution were analyzed directly without workup by ^{2}H NMR spectroscopy. Mass spectrometric characterization of EDA activation by metal complexes was performed by direct injection of reaction solutions.

2.8. X-ray crystallography

Diffraction-quality crystals of $[Mn(R,R\text{-}L^1)(NCMe)_3](ClO_4)_2\cdot MeCN$ were grown by slow diffusion of Et_2O vapor onto a concentrated CH_3CN solution at room temperature. The structure was determined during the 2007 Summer Crystallography School at the University of California San Diego Small Molecule Crystallography Facility, directed by Professor Arnold L. Rheingold (M.P.J.). A pale yellow block (0.20 × 0.20 × 0.20 mm) was mounted on a Bruker SMART APEX CCD diffractometer and data were collected at T = 100(2) K using Mo Kα (λ = 0.71073 Å). The SMART program package was used to determine unit cell parameters and collect data [29]. The raw frame data were processed using SAINT and a multiscan absorption correction was applied by SADABS [29]. Data preparation was carried out using XPREP [29]. The structure was refined in the noncentrosymmetric tetragonal space group $P4_1$ (No. 76). The structure was solved using direct methods and difference Fourier techniques using SHELXTL [30]. All non-hydrogen atoms were located and refined anisotropically, with hydrogen atoms introduced into ideal positions. An R,R configuration was imposed on the chiral diimine backbone carbons, yielding a Flack parameter of 0.01(2) [31]. Details of the refinement and crystal data are summarized in Table 1. Pertinent bond lengths and angles are summarized in Table 2.

Diffraction-quality crystals of $[Mn(R,R\text{-}L^2)(OH_2)_2](ClO_4)_2$ were grown by vapor diffusion of Et_2O onto a concentrated CH_3CN solution. The structure was determined at West Virginia University (J.L.P.) A suitable crystal was washed with the perfluoropolyether PFO-XR75 (Lancaster) and wedged in a glass capillary. The sample was optically aligned on the four-circle of a Siemens P4 diffractometer equipped with a graphite monochromator, a monocap collimator, a Mo Kα radiation source (λ = 0.71073 Å), and a SMART CCD detector held at 5.082 cm from the crystal. Four sets of 20 frames each were collected using the ω scan method and with a 10 s exposure time. Integration of these frames followed by reflection indexing and least-squares refinement produced a crystal orientation matrix for the monoclinic crystal lattice. The program SMART (version 5.6) [29] was used for diffractometer control, frame scans, indexing, orientation matrix calculations, least-squares refinement of cell parameters, and the data collection. Raw data frames were read by the program SAINT (version 5/6.0) [29] and integrated using 3D profiling algorithms. A semi-empirical absorption correction was applied using the SADABS routine available in SAINT [32]. The data were corrected for Lorentz and polarization effects. No evidence of crystal decomposition was observed. Data preparation was carried out by using the program XPREP [29]. The space group was determined to be noncentrosymmetric monoclinic $P2_1$ (No. 4). The structure was solved by a combination of direct methods and difference Fourier analysis with the use of SHELXTL 6.1 [30]. During the course of the refinement, it became apparent that the perchlorate anion containing Cl(1), O(1), O(2), O(3), and O(4) exhibits a two-site disorder (roughly 50:50). The two sites were refined with the eight independent Cl–O distances restrained to 1.44 ± 0.02 Å. The hydrogen atom positions of the two water molecules bound to the Mn were refined with the four O–H distances restrained to 0.90 ± 0.02 Å and the isotropic temperature factor for these hydrogens set at 1.5 times that of the adjacent oxygen atom. Idealized positions for the remaining hydrogen atoms were included as fixed contributions using a riding model with isotropic temperature factors set at 1.2 (aromatic, methylene, and methine protons) or 1.5 (methyl protons) times that of the adjacent carbon atom. The positions of the methyl hydrogen atoms were optimized by a rigid rotating group refinement with idealized tetrahedral angles. A correction for secondary extinction was not applied. The linear absorption coefficient, atomic scattering factors, and anomalous dispersion corrections were calculated from values found in the International Tables of X-ray crystallography [33]. Details of the refinement and crystal data are summarized in Table 1. Pertinent bond lengths and angles are summarized in Table 2. The value of the Flack parameter was 0.08(2) [31].

Crystals of racemic $[Mn(L^3)Cl_2]\cdot 2CH_3OH$ were grown by Et_2O vapor diffusion onto a concentrated MeOH solution. The structure was determined in Leipzig (P.L.). A suitable crystal was washed in perfluoropolyalkyl ether and mounted on an Oxford Diffraction

Table 1
Crystal and refinement data.

Complex	$[Mn(R,R\text{-}L^1)(NCCH_3)_3](ClO_4)_2\cdot CH_3CN$	$[Mn(R,R\text{-}L^2)(OH_2)_2](ClO_4)_2$	$[Mn(L^3)Cl_2]\cdot 2CH_3OH$	$[Mn(L^4)Cl_2]\cdot 2CH_2Cl_2$	$[Mn(L^5)Cl_2]$
Empirical formula	$C_{34}H_{34}Cl_2MnN_8O_8$	$C_{20}H_{28}Cl_2MnN_4O_{10}$	$C_{20}H_{28}Cl_2MnN_4O_2$	$C_{31}H_{37}Cl_6FeMnN_4P$	$C_{12}H_{17}Cl_2MnN_3$
Formula weight	808.53	610.30	482.30	820.11	329.13
T (K)	100(2)	293(2)	130(2)	130(2)	130(2)
Crystal system	tetragonal	monoclinic	monoclinic	triclinic	triclinic
Space group	$P4_1$ (No. 76)	$P2_1$ (No. 4)	$C2/c$ (No. 15)	$P\bar{1}$ (No. 2)	$P\bar{1}$ (No. 2)
a (Å)	8.9191(3)	8.9555(6)	13.0496(9)	13.2451(5)	8.5036(4)
b (Å)	8.9191(3)	11.1432(8)	11.2871(1)	15.8625(6)	8.5597(4)
c (Å)	45.715(3)	13.794(1)	16.3525(9)	17.4514(5)	10.0229(3)
α (°)	90	90	90	75.636(3)	98.400(3)
β (°)	90	93.486(1)	113.400(1)	83.138(3)	97.352(3)
γ (°)	90	90	90	87.361(3)	93.513(4)
V (Å^3)	3636.7(3)	1374.0(2)	2210.5(2)	3526.0(2)	713.41(5)
Z	4	2	4	4	2
Density (calc, g/cm^3)	1.477	1.475	1.449	1.545	1.532
Absorption coefficient (cm^{-1})	5.73	7.32	8.63	12.98	12.85
Crystal size (mm)	0.20 × 0.20 × 0.20	0.12 × 0.32 × 0.38	0.40 × 0.20 × 0.10	0.10 × 0.10 × 0.05	0.20 × 0.05 × 0.05
Reflections	17 592	8851	15 149	74 683	18 158
Independent (R_{int})	5684 (0.0380)	5880 (0.0296)		14 420 (0.1145)	4355 (0.0500)
Data/restraints/parameters	5684/1/482	5880/13/394	15 149/5/187	14 420/4/809	4355/21/225
R_1 [$I > 2\sigma(I)$]	0.0362	0.0457	0.0359	0.0437	0.0354
wR_2 [$I > 2\sigma(I)$]	0.0774	0.1081	0.0771	0.0696	0.0603
R_1 (all data)	0.0407	0.0533	0.0538	0.1172	0.0790
wR_2 (all data)	0.0794	0.1118	0.0815	0.0793	0.0658
Goodness-of-fit (GOF)	1.036	1.005	0.917	0.767	0.845
Difference peak, hole (e Å^{-3})	0.352, −0.322	0.384, −0.259	1.814, −0.271	0.660, −0.673	0.367, −0.326

Table 2
Summary of coordinate bond lengths (Å) and angles (°), with ESDs.

Complex	$[Mn(L^1)(NCMe)_3](ClO_4)_2$	$[Mn(L^2)(OH_2)_2](ClO_4)_2$	$[Mn(L^3)(Cl)_2]$ (major)	$[Mn(L^3)(Cl)_2]$ (minor)	$[Mn(L^4)(Cl)_2]$[b]	$[Mn(L^4)(Cl)_2]$[b]	$[Mn(L^5)(Cl)_2]$ (major)	$[Mn(L^5)(Cl)_2]$ (minor)
Bond lengths (Å)								
Mn–N1 (py, left)[a]	2.446(3)	2.382(2)	2.3767(8)	2.3767(8)	[c]	[c]	2.302(2)	2.302(2)
Mn–N2 (imine, left)[a]	2.314(3)	2.239(3)	2.299(3)	2.247(7)	2.366(3)	2.393(3)	2.207(4)	2.213(9)
Mn–N3 (imine, right)[a]	2.318(3)	2.246(2)	2.299(3)	2.247(7)	2.251(3)	2.252(3)	2.253(1)	2.253(1)
Mn–N4 (py, right)[a]	2.465(3)	2.406(3)	2.3767(8)	2.3767(8)	2.345(3)	2.324(3)	[c]	[c]
Mn–X (ax, top)[a]	2.217(3)	2.136(3)	2.4557(3)	2.4557(3)	2.328(3)	2.288(3)	2.3524(6)	2.3524(6)
Mn–X (ax, bottom)[a]	2.254(3)	2.147(2)	2.4557(3)	2.4557(3)	2.465(1)	2.452(1)	2.3630(6)	2.3630(6)
Mn–X (eq)	2.419(3)	[c]	[c]	[c]	2.436(1)	2.458(2)	[c]	[c]
Bond angles (°)								
N1–Mn–N2	68.64(9)	71.1(1)	70.21(7)	69.4(2)			71.6(1)	71.4(2)
N1–Mn–N3	134.6(1)	139.6(1)	137.90(7)	138.7(2)			145.15(5)	145.15(5)
N1–Mn–N4	155.98(9)	148.2(1)	151.53(4)	151.53(4)				
N2–Mn–N3	69.41(9)	72.05(9)	69.8(1)	71.3(3)	73.6(1)	72.5(1)	75.6(1)	73.8(2)
N2–Mn–N4	134.84(9)	140.6(1)	137.90(7)	138.7(2)	138.8(1)	138.7(1)		
N3–Mn–N4	68.99(9)	70.8(1)	70.21(7)	69.4(2)	70.4(1)	70.8(1)		
X(ax,top)–Mn–N1	94.38(9)	88.9(1)	84.30(3)	84.30(3)			100.64(4)	100.64(4)
X(ax,top)–Mn–N2	81.5(1)	96.9(1)	103.25(6)	117.2(2)	69.7(1)	69.9(1)	106.0(1)	120.7(2)
X(ax,top)–Mn–N3	95.9(1)	111.4(1)	117.46(6)	103.1(2)	92.1(1)	91.3(1)	99.28(4)	99.28(4)
X(ax,top)–Mn–N4	86.08(9)	84.9(1)	83.82(3)	83.82(3)	92.2(1)	92.6(1)		
X(ax,bottom)–Mn–N1	87.15(9)	81.55(9)	83.82(3)	83.82(3)			94.97(4)	94.97(4)
X(ax,bottom)–Mn–N2	117.46(9)	113.8(1)	117.46(6)	103.1(2)	87.53(8)	86.58(8)	138.49(9)	124.0(2)
X(ax,bottom)–Mn–N3	97.21(9)	98.9(1)	103.25(6)	117.2(2)	87.65 (8)	90.17(8)	102.04(5)	102.04(5)
X(ax,bottom)–Mn–N4	84.52(9)	84.6(1)	84.30(3)	84.30(3)	109.91(7)	111.66(8)		
X(ax)–Mn–X(ax)	159.9(1)	142.3(1)	130.21(2)	130.21(2)	156.28(9)	154.69(9)	115.11(2)	115.11(2)
X(eq)–Mn–N1	77.2(1)							
X(eq)–Mn–N2	138.61(9)				119.13(8)	125.65(8)		
X(eq)–Mn–N3	148.23(9)				164.35(9)	159.71(9)		
X(eq)–Mn–N4	79.39(9)				94.42(9)	88.95(9)		
X(eq)–Mn–X(ax,top)	78.5(1)				84.75(8)	87.77(9)		
X(eq)–Mn–X(ax,bottom)	82.3(1)				101.40(4)	99.25(4)		

[a] Directionality is defined from a viewpoint at the middle of the equatorial plane opposite the cyclohexyl ring.
[b] Two independent molecules, with N1 pyridine donor displaced to the "axial, top" positions due to "left" N2 imine reduction.
[c] Vacant site.

Xcalibur S diffractometer equipped with a CCD detector. Data collection and processing, including multi-scan absorption correction, were carried out using the Oxford CRYSALIS software package [34]. The centrosymmetric monoclinic space group $C2/c$ was selected on the basis of systematic absences and the racemic nature of the complex. The structure was solved by direct methods and difference Fourier techniques using SHELXS-97 [35] and refined using SHELXL-97 [36]. The crystal was found to be a merohedral twin (twin matrix by rows: $\bar{1}\,0\,0$, $0\,\bar{1}\,0$, $1\,0\,1$; domain ratio 0.77:0.23). The complex occupies a special position on a two-fold axis; only half of the complex and one full methanol molecule are unique. Moreover, both enantiomers occupy this position in slightly different conformations in a ratio of 0.712(4):0.288(4). All hydrogen atoms were placed in ideal positions, except H1, H3, H4 and H10. Details of the refinement and crystal data are summarized in Table 1. Pertinent bond lengths and angles are summarized in Table 2.

Crystals of racemic $[Mn(L^4)Cl_2]\cdot 2CH_2Cl_2$ were grown by diffusion of layered *n*-hexane into a CH_2Cl_2 solution at −20 °C. The structure was solved in Leipzig (S.T.) using the same equipment and techniques already described (*vide supra*). The centrosymmetric triclinic space group $P\bar{1}$ (No. 2) was determined. Distinct lattice sites were occupied by independent molecules of one enantiomer, differing primarily in orientation of the ferrocenylmethyl moiety. All hydrogen atoms were placed in ideal positions except for N–H and P–H, and these bond lengths were constrained to ideal values. Details of the refinement and crystal data are summarized in Table 1. Pertinent bond lengths and angles are summarized in Table 2.

Crystals of racemic $[Mn(L^5)Cl_2]$ were grown by Et_2O vapor diffusion onto a solution of the complex in MeOH. The structure was solved in Leipzig (S.T.) using the same equipment and techniques already described (*vide supra*). The centrosymmetric triclinic space group $P\bar{1}$ (No. 2) was determined. A single lattice site is occupied by both enantiomers in slightly different conformations in a 0.669(4):0.331(4) ratio. All hydrogen atoms were placed in ideal positions except H2–H5 on the pyridine ring. Details of the refinement and crystal data are summarized in Table 1. Pertinent bond lengths and angles are summarized in Table 2.

3. Results and discussion

3.1. Background and general remarks

Three di-Schiff base ligands were initially explored in the present work (L^1–L^3, Scheme 1). The coordination chemistry of L^1 and L^2 has been scarcely explored. Only bimetallic Cu(I) complexes have been structurally characterized for L^2 and a bis(quinolyl) analog of L^1, with both ligands found in a common bridging bis-bidentate (*i.e.*, μ_2-κ^2,κ^2) mode [20,37]. Additionally, a few asymmetric reactions catalyzed by structurally undefined transition metal and lanthanide complexes of these ligands have been reported [17–20], but none of these involved manganese. L^3 has been more widely exploited. Six-coordinate $[Mn(L^3)(ClO_4)_2]$ [6] and $[Mn(L^3)Br_2]$ [8], seven-coordinate $[Mn(L^3)(OH_2)_2Br]Br$ [8] and eight-coordinate $[Mn(L^3)(\kappa^2\text{-}OAc)_2]$ [13] structures have all been characterized, as have manganese(II) complexes of several closely related ligands [8,10,11–13]. Some of these have been utilized as catalysts for asymmetric sulfoxidation [6], olefin epoxidation [12], and olefin polymerization [7].

In the present work, we prepared several manganese(II) complexes of L^1–L^3. L^1 and L^2 were prepared as enantiopure *R*,*R* isomers, while L^3 was prepared both as a racemate and as enantiopure *R*,*R* and *S*,*S*-isomers. These were added to $Mn(ClO_4)_2\cdot 6H_2O$ to prepare the manganese(II) complex salts. Since [Mn

(S,S-L^3)$(ClO_4)_2$] has already been reported [6], we also prepared a neutral dichloride complex from $MnCl_2{\cdot}4H_2O$. The racemic L^3 complexes were then reacted with either the primary phosphine $FcCH_2PH_2$ or ethyldiazoacetate (EDA) as phosphinidene or carbene precursors, respectively. Instead of metal-centered chemistry, selective ligand modification occurred in both cases, yielding new complexes of ligand derivatives L^4 and L^5 (Scheme 1) that result from respective hydrophosphination or hydrolysis of a single electrophilic imine bond.

3.2. X-ray crystallography of manganese(II) complexes of L^1–L^3

Structures of isolated manganese(II) complexes of L^1–L^3 are shown in Fig. 1. Coordinate bond lengths and angles are summarized in Table 2, which retains the perspective shown in Fig. 1 (*i.e.*, the axial, top donor listed for the L^1 complex in the table is N7 of the coordinated acetonitrile molecule shown at the top of the structure in the figure). The first complex, [Mn(R,R-L^1)$(NCCH_3)_3$]$(ClO_4)_2{\cdot}CH_3CN$ is distinguished by its heptacoordinate, approximately pentagonal bipyramidal ligand field, which includes the tetradentate di-Schiff base ligand and three acetonitrile solvent molecules. The fourth acetonitrile molecule and the perchlorate counteranions are tightly packed with the complex cation, but clearly reside outside the primary coordination shell. Pentagonal bipyramidal manganese(II) is uncommon but not unprecedented [38]; examples particularly relevant to the structure at hand are [Mn(L^3)$(OH_2)_2$Br]Br [9], several closely related Schiff base ligands [10–12], a bis(2-pyridylmethyl)-1,4-diazepane ligand complex [39], and several pentaazamacrocycle complexes [40–42].

A pentagonal plane is particularly accommodated by the constrained tetradentate ligand bite of L^1. Compared to dianionic salen ligands with exocyclic phenolate oxygen donor atoms that give two outer six-atom and one inner five-atom chelate rings, with averaged O–Mn–N and N–Mn–N *cis* angles of 91(2)° and 82(1)°, respectively [43], the neutral pyridylmethylidene donors afford three contiguous five-atom chelate rings. This reduces the *cis* N–Mn–N bite angles to an average value of 69.0(4)° in the L^1 complex (Table 2), thus circumscribing four contiguous vertices on a pentagonal equatorial plane (*i.e.*, 72°). A least-squares plane calculated using the four ligand nitrogens passes through the manganese ion only 0.004 Å off-center; however, the rigid backbone introduces ruffling of the nitrogen array, with respective displacements of ±0.161(1) and ±0.301(1) Å for the pyridyl and imine nitrogens. The pyridines are pinned back to a "trans" angle of 155.98(9)°, and afford somewhat longer Mn–N bonds than the imines (*i.e.*, 2.46(1) versus 2.32(1) Å average).

The fifth equatorial position is occupied by an acetonitrile molecule, but the N6 donor nitrogen is displaced +0.535 Å above the N_4 ligand plane just described, and exhibits a significantly elongated bond compared to the axial acetonitriles (2.419(3) versus 2.254(3) and 2.217(3) Å for Mn1–N6, N5 and N7, respectively). Moreover, the axial N5–Mn1–N7 *trans* angle is reduced to 159.9(1)°, specifically bending toward the equatorial solvent ligand; N5–Mn1–N6 and N7–Mn1–N6 *cis* angles are reduced to 82.3(1)° and 78.5(1)°, respectively. The acetonitrile ligands are otherwise unremarkable. A second least-squares plane passes directly through all three acetonitrile nitrogens, with the manganese ion offset by 0.137 Å toward N1, and this N_3 meridional plane meets the equatorial N_4 plane at nearly a right angle (86.73°). Thus, only minor distortion from a pentagonal bipyramid is evident in $[Mn(L^1)(NCCH_3)_3]^{2+}$, principally entailing ruffling of the L^1 donor plane and elongation of the equatorial acetonitrile coordination.

A similar $[Mn(L)(NCCH_3)_3]^{2+}$ complex was recently reported, with a planar tetradentate supporting ligand and an elongated bond to a coplanar equatorial acetonitrile [39]. Two [Mn(κ^4-L)(κ^2-L)X] structures incorporating similar di-Schiff base dipyridyldiimine ligands display elongated bonds to equatorial pyridines on the tetradentate ligands [9,11]. Also, a number of pentaazamacrocyclic complexes exhibit unusually long bonds to axial co-ligands [40,42]. The disparate distortional modes primarily may reflect differing geometric constraints afforded by diverging chelation within otherwise similar ligand fields [44]. However, while high-spin Mn(II) does not exhibit ligand field stabilization, orbital differentiation of axial and equatorial σ-bonding can exist under pentagonal bipyramidal symmetry [45].

The six-coordinate structures of [Mn(L^2)$(OH_2)_2$]$(ClO_4)_2$ and [Mn(L^3)Cl_2] can be interpreted as monovacant pentagonal bipyramids, with the elongated equatorial site of [Mn(L^1)$(NCCH_3)_3$]$(ClO_4)_2$ remaining unoccupied by an exogenous ligand. In fact, this fifth equatorial site is blocked by the pyridine α-methyl substituents of L^2. As a result, the axial donor atoms bend toward the equatorial site, closing down the *trans* angle between them from 159.9(1)° to 142.3(1)° and 130.21(2)° in the respective complexes. Similar hexacoordinate structures were reported previously for [Mn(L^3)X_2] (X^- = ClO_4^-, Br) [6,8] and the dichloride complex of a bis(quinolyl)-substituted ligand [7]. Hydrogen bonds are evident between the aquo ligand protons in the L^2 complex and outer-sphere perchlorate oxygens (1.86–1.97 Å), and between the chloride ligands of the L^3 complex and a lattice methanol proton (2.47 Å). However, the Mn–OH_2 and Mn–Cl bond lengths are not atypical [43]. The Mn–N bond lengths also vary only slightly between L^2 and the major conformation of L^3, notwithstanding differing charge of the axial co-ligands, but are slightly shorter compared to the heptacoordinate L^1 complex. Rufflings of the N_4 equatorial planes are also moderated: ±0.144 Å for the pyridines and ±0.256 Å for the imines of L^2, and ±0.128 Å for the pyridines and ±0.228 Å for the imines of L^3. The Mn(II) ions reside in this plane, offset by +0.050 and 0.000 Å, respectively, while axial MnX_2 (X = OH_2, Cl^-) planes cross at 88.37° and 87.08°.

3.3. Hydrophosphination of [Mn(L^3)Cl_2]

One equivalent of the air-stable primary phosphine $FcCH_2PH_2$ (Fc = $-C_5H_4FeC_5H_5$) was added to racemic [Mn(L^3)Cl_2], with the goal of preparing an adduct [Eq. (1)] that could be utilized as a phosphinidene precursor [*e.g.*, Eq. (2)] [46,47]. Characterization of

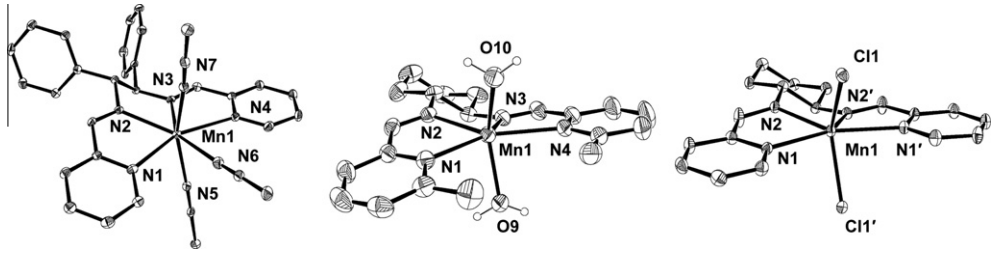

Fig. 1. ORTEP plots (30% ellipsoids) of the complex cations of [Mn(R,R-L^1)$(NCCH_3)_3$]$(ClO_4)_2{\cdot}CH_3CN$ (left) and [Mn(R,R-L^2)$(OH_2)_2$]$(ClO_4)_2$ (center), as well as the major conformation of the neutral racemic complex [Mn(L^3)Cl_2]$\cdot 2CH_3OH$ (right), arbitrarily depicted as the R,R-enantiomer. Hydrogen atoms (other than H_2O) were omitted for clarity.

the product by electrospray ionization mass spectrometry gave clear evidence of adduct formation. A parent ion was observed with a mass/charge ratio of 614.1 amu, compared to a calculated exact mass of 614.09 amu for $[Mn(L^4)Cl]^+$. Moreover, the isotope pattern was consistent with the presence of one iron and one chlorine atom and the expected ^{13}C distribution (Fig. 2). However, FTIR spectroscopy clearly indicated that phosphine addition occurred at the electrophilic imine bond instead of metal ligation [Eq. (3)], forming a complex of a reduced monoamine ligand (L^4, Scheme 1). This was indicated clearly by attenuation of the corresponding

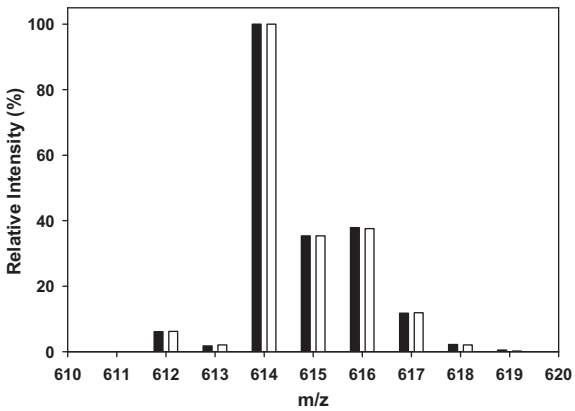

Fig. 2. Observed (black) and calculated (white) isotope pattern for the parent ion of the addition product $[Mn(L^3)Cl{\cdot}PH_2CH_2Fc]^+$, observed by electrospray ionization mass spectrometry.

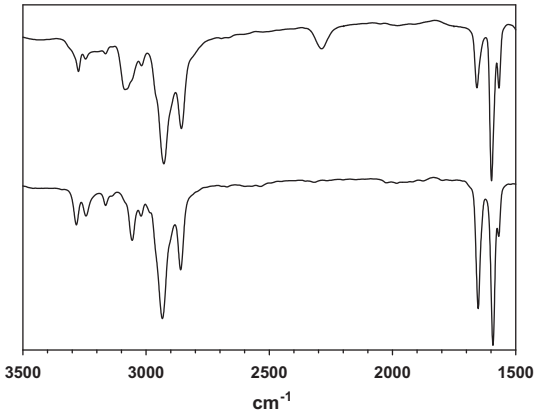

Fig. 3. Excerpts of FTIR spectra for $[Mn(L^3)Cl_2]$ (bottom) and the $FcCH_2PH_2$ addition product (top), illustrating (from high to low energy) new ν(C–H) and ν(P–H) modes and attenuation of the imine ν(C=N) mode.

ν(C=N) mode at 1658 cm^{-1} (Fig. 3). A ν(P–H) band at 2288 cm^{-1} was unshifted from that of the free phosphine precursor [21], consistent with absence of metal ligation [48]. New modes in the ν(C–H) region due to the ferrocenylmethyl substituent were also evident. Addition of a second phosphine equivalent did not result in further alteration of the FTIR spectra even after prolonged reflux.

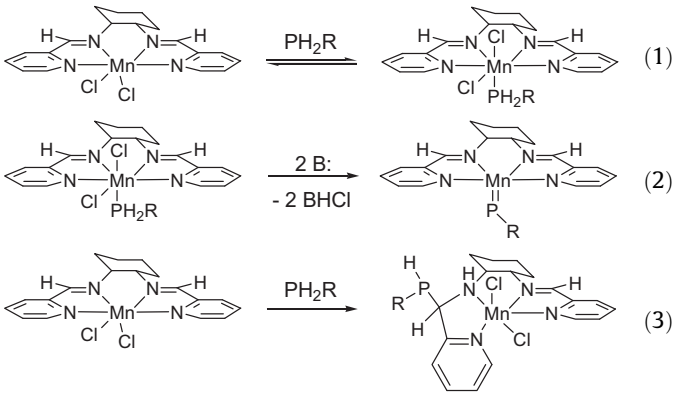

The novel hydrophosphination product complex $[Mn(L^4)Cl_2]$ was further characterized by X-ray crystallography, which revealed details of the imine reduction. Two independent molecules were observed that differ only trivially in the orientation of their respective ferrocenylmethyl substituents, which are unremarkable (Fig. 4). Imine reduction forces refolding of the ligand from the planar configuration of L^3 into a *cis*-β geometry [49], with the pyridine on the reduced arm displaced to an axial position and the other retained in the equatorial plane. Diastereoselectivity of the product complex must be determined by the preexisting chirality imposed by the cyclohexyl backbone. Addition of $FcCH_2PH_2$ to the *R*,*R*-enantiomer of $[Mn(L^3)Cl_2]$ occurred at the imine *si* face to extend chirality across the imine bond, yielding *S*-carbon and *R*-nitrogen. This was reversed at the *S*,*S*-enantiomer. The selectivity results from folding of the reduced pyridinylmethyl arm into an equatorial position on the amine nitrogen, which is locked by fusion of two five-atom chelate rings. Addition to the opposite face would thus entail formation of a minor axial diastereomer, but its relative yield was not determined.

Approximate pentagonal bipyramidal geometry is still maintained, with one open equatorial site vacated by the displaced pyridine. The chlorides are retained in *cis*-equatorial and *trans*-axial positions, with nearly equal bond lengths, approaching those of the $[Mn(L^3)Cl_2]$ precursor. However, the equatorial chloride bends approximately 20° toward the open equatorial site, so the equatorial Cl–Mn–N angles to the pyridine and amine, respectively, average 92(4)° and 122(5)° in both unique molecules, compared to the ideal 72° and 144°. Owing to the constrained pyridylmethyl arm, the axial *trans* angle from the second chloride to the pyridine aver-

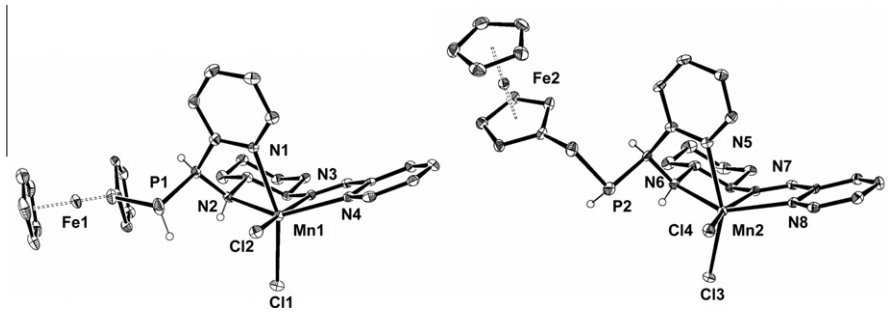

Fig. 4. ORTEP drawings (30% ellipsoids) of the two independent molecules of $[Mn(L^4)Cl_2]$, arbitrarily depicted as *R*,*R*-enantiomer. Hydrogen atoms are omitted for clarity, except those relating to the reduced imine bond.

ages 155(1)°, while the N–Mn–Cl and Cl–Mn–Cl *cis* angles average 86(2)° and 100(1)°, respectively. The axial pyridine bond length is 0.07(3) Å shorter in the *cis*-β L^4 configuration than in the precursor, while the equatorial amine bond is markedly lengthened compared to the imine. The imine C=N bond averages 1.264(4) Å in the two L^4 complexes, compared to 1.277(3) Å in the major isomer of the L^3 precursor complex, and 1.474(4) Å for the reduced amine C–N bond.

3.4. Reaction of $[Mn(L^3)(X)_2]$ with EDA

We also investigated reactivity of the L^3 complexes with ethyldiazoacetate (EDA) as a carbene precursor. Addition of EDA to a dilute solution of $[Mn(L^3)(ClO_4)_2]$ in CH_3CN produced no obvious effervescence. Monitoring of the reaction solution by electrospray mass spectrometry, in the absence of a convenient solution-phase spectroscopic probe, gave evidence of EDA activation upon extended thermolysis. The parent ion corresponding to $[Mn(L^3)ClO_4]^+$ at 446 amu was observed along with heavier ions consistent with carbene addition. Using a mixture of ordinary and d_5-EDA enriched on the ethyl substituent, a pair of product ions were observed at 468 and 473 amu, consistent with assignment as a carbene adduct $[Mn(L^3)(OH_2)(OH)\{C(H)C(O)OEt\}]^+$ (Fig. 5). Prolonged thermolysis resulted in exhaustion of precursor ion at 446 amu and appearance of further derivative peaks at 379 amu and 290 amu, corresponding to consecutive imine hydrolyses with loss of 89 amu (Fig. 6). Reaction of $[Mn(L^3)Cl_2]$ with EDA gave analogous peaks at 382 amu, corresponding to $[Mn(L^3)Cl]^+$, and 468 amu, corresponding to $[Mn(L^3)Cl\{C(H)C(O)OEt\}]^+$ (Fig. 7).

The various ions produced from $[Mn(L^3)(ClO_4)_2]$ were further probed by selective ion trapping and fragmentation by collision-induced dissociation (CID). Both the normal and d_5-enriched product ions at 468 and 473 amu gave a common major fragment at 365 amu, consistent with $[Mn(L^3)(OH_2)]^+$. In contrast, the imine-hydrolyzed ions at 379 and 290 amu gave major fragmentation products with mass losses of 46 amu, implying loss of EtOH to form ketenylidene (*i.e.*, C=C=O); this was also confirmed by CID fragmentation of the d_5-enriched peak at 384 amu with loss of 51 amu. The various derivative ions are summarized in Scheme 2, in which complex geometries are arbitrary and formation of a metallocarbene is assumed, rather than Mn–N bond insertion, due to observation of ions with hydrolyzed imine linkages.

As a test for EDA activation in solution, excess styrene was added to capture any incipient carbenoid fragment. Cyclopropane formation (29% yield, 1.0:1.7 *syn:anti*) was observed, along with

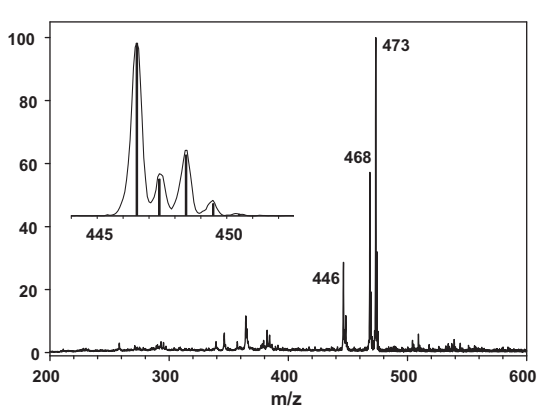

Fig. 5. ESI mass spectrum for reaction of $[Mn(L^3)(ClO_4)_2]^+$ with a mixture of ordinary and d_5-labeled EDA in CH_3CN. Inset shows the parent ion of the complex cation obtained in the absence of EDA at 446 amu, with the theoretical isotope distribution indicated by vertical bars.

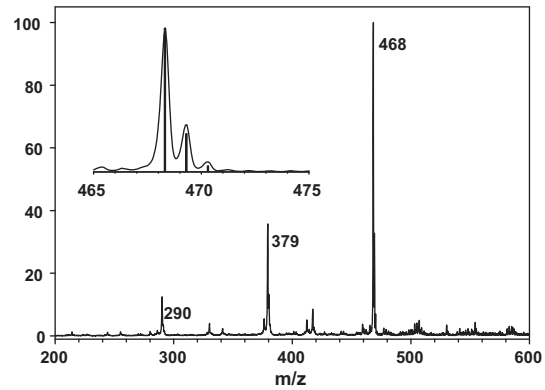

Fig. 6. ESI mass spectrum for prolonged reaction of $[Mn(L^3)(ClO_4)_2]^+$ with EDA in CH_3CN. Inset shows the parent ion for the product cation $[Mn(L^3)(OH_2)(OH)\{C(H)C(O)OEt\}]^+$ at 468 amu, with the theoretical isotope distribution indicated by vertical bars.

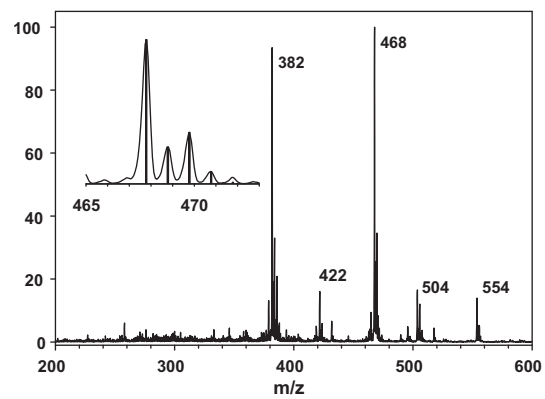

Fig. 7. ESI mass spectrum for reaction of $[Mn(L^3)Cl_2]$ with EDA in CH_3CN. Inset shows the parent ion for the product cation $[Mn(L^3)Cl\{C(H)C(O)OEt\}]^+$ at 468 amu, with the theoretical isotope distribution indicated by vertical bars.

the minor insertion product *cis*-ethyl-4-phenyl-3-butenoate. However, several lines of evidence indicated a lack of significant metal-catalyzed carbene transfer: (i), in the absence of catalyst, a significant yield (54%) of 3-carboxy-5-phenyl-2-pyrazoline ethyl ester was observed by ^1H NMR spectroscopy, consistent with direct 1,3-dipolar addition of EDA to styrene; (ii), the reaction timescale was consistent with known rates for such a reaction [50]; (iii), olefinic carbene coupling products (*i.e.*, diethylmaleate and fumarate) were not observed; (iv), cyclopropanes still formed in the absence of catalyst; and (v), chiral induction into the cyclopropanes was not observed in the presence of a single L^3 complex enantiomer. Thus, we conclude that the $[Mn(L^3)X_2]$ complexes were not active as carbene transfer catalysts, at least under the conditions utilized in the present study (*vide supra*).

3.5. Reaction of $[Mn(L^3)Cl_2]$ with H_2O

Extended thermolysis of $[Mn(L^3)Cl_2]$ with EDA also engendered a deep orange color in solution, which we attributed to reversible imine bond hydrolysis [Eq. (4)]. Water was added to a yellow solution of $[Mn(L^3)Cl_2]$ in methanol to afford orange crystals upon ether vapor diffusion. Elemental analysis and X-ray crystallography confirmed the formulation of the orange derivative complex as $[Mn(L^5)Cl_2]$, where L^5 is the tridentate hydrolysis product of one imine linkage of L^3 (Fig. 8). The structure of $[Mn(L^5)Cl_2]$ is interesting insofar as penta-coordinate manganese(II) complexes

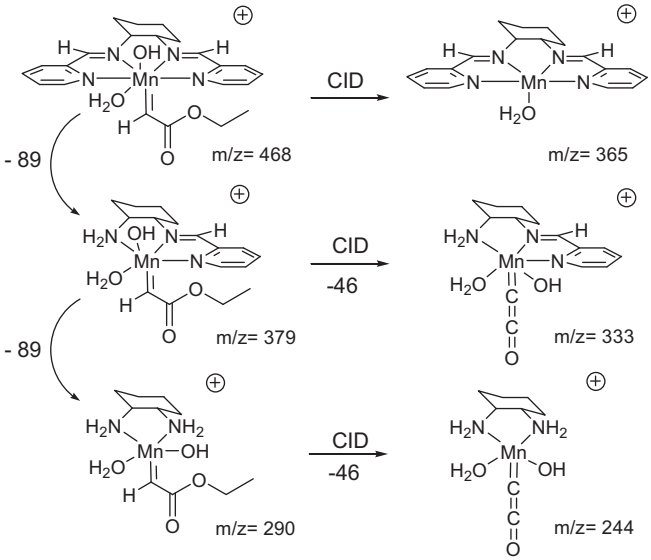

Scheme 2.

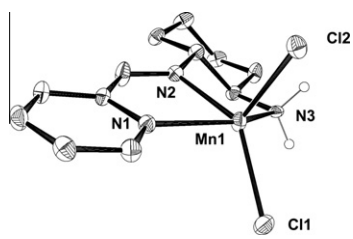

Fig. 8. ORTEP diagram (30% ellipsoids) of the major conformation of $[Mn(L^5)Cl_2]$, arbitrarily shown as the *R*,*R*-enantiomer. Hydrogen atoms are omitted for clarity, except for the amine.

are comparatively rare [51,52]. The structure can be viewed as an equatorially *cis*-divacant pentagonal bipyramid, with axial chlorides bent toward the open sites and the Cl–Mn–Cl angle accordingly reduced to 115.11(2)°. More conventionally, a square pyramidal structure can be assigned, with "*trans*" angles in the equatorial plane of 145.15(5)° from the remaining pyridine (N1) to the amine (N3), and 138.49(9)° from the imine nitrogen (N2) to Cl1 in the major conformation. This gives a τ value of 0.11 [53]. The three remaining N–Mn–Cl angles to the axial Cl2 average 102(4)°. All five metal–ligand bond lengths are shorter than their counterparts in the hexacoordinate $[Mn(L^3)Cl_2]$ (Table 2).

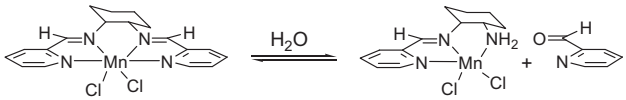

(4)

4. Summary and conclusions

Inspired by the use of di-Schiff base pyridylmethylidene manganese(II) complexes for catalysis of stereoselective oxo atom transfer and olefin polymerization, we prepared a series of three ligand complexes and investigated their potential for transfer catalysis of soft isolobal oxene analogues, including an air-stable primary phosphine as a phosphinidene precursor and ethyldiazoacetate as a carbene precursor. However, the reactive ligand imine bonds instead yielded respective hydrophosphination and hydrolysis reactions. Such reactivity can be expected to constrain the use of these complexes as group transfer catalysts. Imine reduction would overcome these limitations, but also enable a high degree of conformational flexibility, as demonstrated previously [49,54] and illustrated again by the L^4 complex herein. Nonetheless, we did obtain novel ligand derivatives L^4 and L^5, and X-ray crystallographic studies of the L^1–L^5 complexes gave a series of five-, six- and seven-coordinate structures related by the pentagonal bipyramidal geometry imposed by ligand constraints in the equatorial plane.

Acknowledgments

We thank Professor Arnold Rheingold for his invitation to the Summer Crystallography School at UCSD. This work was supported by startup funds provided by Ohio University (M.P.J.), and by a grant from the US National Science Foundation (G.P.J., DBI-0648757). We also thank the Ohio University Office of the Vice President for Research for its support of the Chemistry and Biochemistry at the Materials Interface Exchange Program with the University of Leipzig.

Appendix A. Supplementary material

CCDC 645115 contains the supplementary crystallographic data for this paper. These data can be obtained free of charge from The Cambridge Crystallographic Data Centre via www.ccdc.cam.ac.uk/data_request/cif. Supplementary data associated with this article can be found, in the online version, at doi:10.1016/j.ica.2010.06.041.

References

[1] B.M. Trost, Proc. Natl. Acad. Sci. USA 101 (2004) 5348.
[2] P.G. Cozzi, Chem. Soc. Rev. 33 (2004) 410.
[3] K. Srinivasan, P. Michaud, J.K. Kochi, J. Am. Chem. Soc. 108 (1986) 2309.
[4] W. Zhang, J.L. Loebach, S.R. Wilson, E.N. Jacobsen, J. Am. Chem. Soc. 112 (1990) 2801.
[5] R. Irie, K. Noda, Y. Ito, N. Matsumoto, T. Katsuki, Tetrahedron Lett. 31 (1990) 7345.
[6] S. Schoumacker, O. Hamelin, J. Pécaut, M. Fontecave, Inorg. Chem. 42 (2003) 8110.
[7] K. Yliheikkilä, K. Axenov, M.T. Räisänen, M. Klinga, M.P. Lankinen, M. Kettunen, M. Leskelä, T. Repo, Organometallics 26 (2007) 980.
[8] I.-C. Hwang, K. Ha, Acta Crystallogr. E 63 (2007) m2465.
[9] X.-M. Ouyang, B.-L. Fei, T.-A. Okamura, W.-Y. Sun, W.-X. Tang, N. Ueyama, Chem. Lett. (2002) 362.
[10] T.K. Karmakar, B.K. Ghosh, A. Usman, H.-K. Fun, E. Rivière, T. Mallah, G. Aromí, S.K. Chandra, Inorg. Chem. 44 (2005) 2391.
[11] T.K. Karmakar, G. Aromí, B.K. Ghosh, A. Usman, H.-K. Fun, T. Mallah, U. Behrens, X. Solans, S.K. Chandra, J. Mater. Chem. 16 (2006) 278.
[12] M. Louloudi, V. Nastopoulos, S. Gourbatsis, S.P. Perlepes, N. Hadjiliadis, Inorg. Chem. Commun. 2 (1999) 479.
[13] I.-C. Hwang, K. Ha, Acta Crystallogr. E 64 (2008) m453.
[14] H.-H. Liu, Y. Wang, Y.-J. Shu, X.-G. Zhou, J. Wu, S.-Y. Yan, J. Mol. Catal. A 246 (2006) 49.
[15] J. Gao, F.R. Woolley, R.A. Zingaro, Org. Biomol. Chem. 3 (2005) 2126.
[16] V.B. Sharma, S.L. Jain, B. Sain, Catal. Lett. 94 (2004) 57.
[17] R. ter Halle, A. Bréhéret, E. Schulz, C. Pinel, M. Lemaire, Tetrahedron: Asymmetr. 8 (1997) 2101.
[18] Y.-G. Li, Q.-S. Tian, J. Zhao, Y. Feng, M.-J. Li, T.-P. You, Tetrahedron: Asymmetr. 15 (2004) 1707.
[19] C.I. Maxwell, K. Shah, P.V. Samuleev, A.A. Neverov, R.S. Brown, Org. Biomol. Chem. 6 (2008) 2796.
[20] V. Amendola, L. Fabbrizzi, L. Gianelli, C. Maggi, C. Mangano, P. Pallavicini, M. Zema, Inorg. Chem. 40 (2001) 3579.
[21] N.J. Goodwin, W. Henderson, B.K. Nicholson, J. Fawcett, D.R. Russell, J. Chem. Soc., Dalton Trans. (1999) 1785.
[22] M.P. Doyle, Chem. Rev. 86 (1986) 919.
[23] J.E. Baldwin, C.G. Carter, J. Am. Chem. Soc. 104 (1982) 1362.
[24] Y. Fu, F.L. King, D.C. Duckworth, J. Am. Soc. Mass Spectr. 17 (2006) 939.
[25] D.F. Evans, D.A. Jakubovic, J. Chem. Soc., Dalton Trans. (1988) 2927.
[26] Y. Chen, K.B. Fields, X.P. Zhang, J. Am. Chem. Soc. 126 (2004) 14718.
[27] K. Takami, H. Yorimitsu, K. Oshima, Org. Lett. 6 (2004) 4555.
[28] ^{1}H NMR data (δ, ppm in $CDCl_3$): 1.39 (3H, t, 7.1 Hz); 2.97 (1H, dd, 17.3, 9.3 Hz); 3.41 (1H, dd, 17.3, 11.8); 4.34 (2H, q, 7.1 Hz); 5.03 (1H, dd, 11.8, 9.3 Hz); 6.44

(1H, s). Data for the methyl ester: W.S. Brey Jr., C.M. Valencia, Can. J. Chem. 46 (1968) 810.
[29] SMART, SAINT, and SADABS, Bruker, Madison, 2000.
[30] G.M. Sheldrick, SHELXTL6.1, Bruker AXS, Madison, 2000.
[31] H.D. Flack, Acta Crystallogr. A 39 (1983) 876.
[32] R. Blessing, Acta Crystallogr. A 51 (1995) 33.
[33] International Tables for X-ray Crystallography, vol. IV, Kynoch Press, Birmingham, 1974, p. 55.
[34] SCALE3 ABSPACK, Empirical Absorption Correction, CRYSALIS software package, Oxford Diffraction, Ltd., 2006.
[35] G.M. Sheldrick, SHELXS-97, Program for Crystal Structure Solution, University of Göttingen, 1997.
[36] G.M. Sheldrick, SHELXL-97, Program for Crystal Structure Solution, University of Göttingen, 1997.
[37] V. Amendola, M. Biocchi, Y.D. Fernandez, C. Mangano, P. Pallavicini, Collect. Czech. Chem. Commun. 68 (2003) 1647.
[38] D. Casanova, P. Alemany, J.M. Bofill, S. Alvarez, Chem. Eur. J. 9 (2003) 1281.
[39] R.A. Geiger, S. Chattopadhyay, V.W. Day, T.A. Jackson, J. Am. Chem. Soc. 132 (2010) 2821.
[40] K. Aston, N. Rath, A. Naik, U. Slomczynska, O.F. Schall, D.P. Riley, Inorg. Chem. 40 (2001) 1779.
[41] A.K. Sra, J.-P. Sutter, P. Guionneau, D. Chasseau, J.V. Yakhmi, O. Kahn, Inorg. Chim. Acta 300–302 (2000) 778.
[42] W. Park, M.H. Shin, J.H. Chung, J. Park, M.S. Lah, D. Lim, Tetrahedron Lett. 47 (2006) 8841.
[43] Cambridge Structural Database, v. 5.32, Cambridge Crystallographic Data Centre, 2009; A.G. Orpen, Acta Crystallogr. B 58 (2002) 398.
[44] G.J. Palenik, D.W. Wester, Inorg. Chem. 17 (1978) 864.
[45] R. Hoffmann, B.F. Beier, E.L. Meutterties, A.R. Rossi, Inorg. Chem. 16 (1977) 511.
[46] G.A. Abdul Hadi, K. Fromm, S. Blaurock, S. Jelonek, E. Hey-Hawkins, Polyhedron 16 (1997) 721.
[47] U. Segerer, R. Felsberg, S. Blaurock, G. Abdul Hadi, E. Hey-Hawkins, Phosphorus Sulfur Silicon Relat. Elem. 144–146 (1999) 477.
[48] S.I.M. Paris, J.L. Petersen, E. Hey-Hawkins, M.P. Jensen, Inorg. Chem. 45 (2006) 5561.
[49] M. Costas, L. Que Jr., Angew. Chem., Int. Ed. 41 (2002) 2179.
[50] R. Huisgen, H. Stangl, H.J. Sturm, H. Wagenhofer, Angew. Chem. 73 (1961) 170.
[51] C. Mantel, C. Baffert, I. Romero, A. Deronzier, J. Pécaut, M.-N. Collomb, C. Duboc, Inorg. Chem. 43 (2004) 6455.
[52] C. Baffert, I. Romero, J. Pécaut, A. Llobet, A. Deronzier, M.-N. Collomb, Inorg. Chim. Acta 357 (2004) 3430.
[53] A.W. Addison, T.N. Rao, J. Reedijk, J. van Rijn, G.C. Verschoor, J. Chem. Soc., Dalton Trans. (1984) 1349.
[54] C. Ng, M. Sabat, C.L. Fraser, Inorg. Chem. 38 (1999) 5545.